Edinburgh Research Explorer

A Dense Metal-Organic Framework for Enhanced Magnetic Refrigeration

A Dense Metal-Organic Framework for

Enhanced Magnetic Refrigeration**

Giulia Lorusso,[1] Joseph W. Sharples,[2] Elias Palacios,[1] Olivier Roubeau,[1] Euan K. Brechin,[3]

Roberta Sessoli,[4] Andrea Rossin,[5] Floriana Tuna,[2] Eric J. L. McInnes,[2] David Collison[2]

and Marco Evangelisti[1,*]

[1]Instituto de Ciencia de Materiales de Aragón (ICMA), CSIC − Universidad de Zaragoza, Departamento de Física de la Materia Condensada, 50009 Zaragoza, Spain.

[2]School of Chemistry and Photon Science Institute, The University of Manchester, M13-9PL Manchester, UK.

[3]EaStCHEM, School of Chemistry, Joseph Black Building, University of Edinburgh, West Mains Road, Edinburgh, EH9 3JJ, UK.

[4]Department of Chemistry and INSTM, Università degli Studi di Firenze, 50019 Sesto Fiorentino, Italy.

[5]Istituto di Chimica dei Composti Organometallici (ICCOM), CNR, 50019 Sesto Fiorentino, Italy.

[*]Corresponding author; e-mail: evange@unizar.es; homepage: http://molchip.unizar.es/

Supporting information:
Supporting Information is available from the Wiley Online Library or from the author.

Graphical abstract:
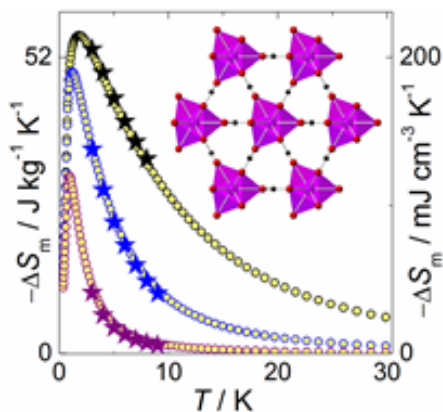
Keywords:
gadolinium formate; metal-organic framework; magnetocaloric effect; magnetic refrigeration; molecule-based magnet

Abstract

The three-dimensional metal-organic framework Gd(HCOO)$_3$ is characterized by a relatively compact crystal lattice of weakly interacting Gd^{3+} spin centers interconnected via lightweight formate ligands, overall providing a remarkably large magnetic:non-magnetic elemental weight ratio. The resulting magnetocaloric effect per unit volume is decidedly superior in Gd(HCOO)$_3$ than in the best known magnetic refrigerant materials for liquid-helium temperatures and low-moderate applied fields.

Main text

Recent years have witnessed a terrific increase in the number of molecule-based materials proposed as magnetic refrigerants for liquid-helium temperatures.[1-15] Refrigeration proceeds adiabatically via the magnetocaloric effect (MCE), which describes the changes of magnetic entropy (ΔS_m) and adiabatic temperature (ΔT_{ad}), following a change in the applied magnetic field (ΔB). As in the first paramagnetic salt that permitted sub-Kelvin temperatures to be reached in 1933,[16] gadolinium is often present because its orbital angular momentum is zero and it has the largest entropy per single ion.[1] The controlled spatial assembly of the Gd^{3+} spin centers is vital for designing the ideal magnetic refrigerant. On the one hand, the magnetic density should be maximized by, for example, limiting the amount of non-magnetic elements which act passively in the physical process. On the other hand, magnetic ordering for $B = 0$ should be avoided, since this results in the decrease of MCE above the target working temperature of the refrigerant. Therefore a compromise becomes necessary, especially for reaching low temperatures.

Metal-Organic Framework (MOF) materials have recently attracted interest for their cooling properties, combined with their synthetic variety and intrinsic robustness.[11-15] Indeed, the dimensionality of Gd-MOFs has no effect in itself on the MCE, bar its intrinsic density. Light and short bridging ligands, such as the formate ion are clearly advantageous in this regard. We therefore focus here on gadolinium formate Gd(HCOO)$_3$, a dense MOF material, characterized by a relatively high packing density of Gd^{3+} ions, linked only through lightweight formate ligands, whose structure was originally determined on powder specimens.[17,18] Surprisingly, no previous magnetic measurements on Gd(HCOO)$_3$ are reported in the literature, except for initial Mössbauer experiments.[19] The single-crystal structure determination of Gd(HCOO)$_3$ is reported here, completing the original powder diffraction study. Our detailed magnetic and thermal studies allow direct and indirect estimation of its MCE and show that, while presenting a sub-Kelvin ordering temperature, Gd(HCOO)$_3$ indeed possesses a huge MCE positioning this material in an enviable position within this research area.

Single crystals of Gd(HCOO)$_3$ were grown by allowing a solution of Gd(NO$_3$)$_3$·5H$_2$O (0.5 g, 1mmol), formic acid (15 mL) and H$_2$O (10 mL) to evaporate slowly over several days. The product was collected as a crystalline solid and dried under vacuum (> 90 % yield) and characterised by elemental analysis for GdC$_3$H$_3$O$_6$: (calculated:found, wt%) Gd 53.80:53.57; C 12.33:12.32; H 1.03:1.07; N none found. The large colorless blocks allowed re-determination of the crystal structure from single-crystal diffraction, and in particular confirmed the crystal system to be hexagonal and the space group $R3m$, with a = 10.4583(4) Å and c = 3.9869(3) Å. The structure of Gd(HCOO)$_3$ describes chains of Gd^{3+} ions propagating along the c axis, each bridged to its neighbors through three μ-formate O-atoms (see **Figure**

1a). These chains are connected in the *bc* plane through the formate ions bridging in μ-O,O' *anti-anti* mode, resulting in the dense hexagonal framework (calculated density is 3.856 g/cm^3) shown in **Figure 1b**. The Gd^{3+} ion is nine-coordinate in an almost perfect tricapped trigonal prismatic environment, with Gd–O distances of 2.496(4) and 2.527(4) Å for the prismatic oxygen O1 and 2.403(4) Å for the capping oxygen O2. The nearest and next-nearest neighbor Gd⋅⋅⋅Gd separations are 3.9869(3) Å within the chains, coinciding with the cell parameter *c*, and 6.183(1) and 6.597(1) Å between chains, respectively.
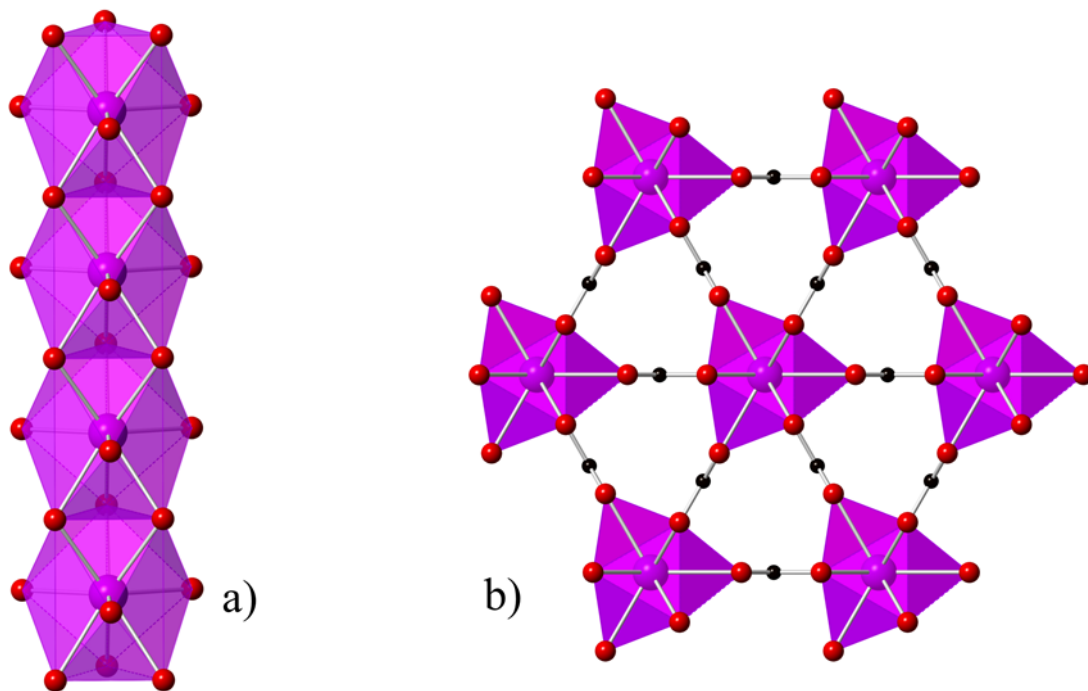

Figure 1. Views of the structure of Gd(HCOO)$_3$ parallel (a) and perpendicular (b) to the *c* axis. Color code: Gd, purple, O, red, C, black. H atoms are omitted for clarity. The 9-coordinate tricapped trigonal prism coordination sphere of Gd^{3+} ions is highlighted.

The molar magnetization *M* was collected for temperatures 2 − 10 K (**Figure S1**). The magnetization saturates to the expected value of 7 μ_B for a Gd^{3+} spin moment, according to which *s* = 7/2 and *g* = 2. The *M(B)* curves can be described well by a Brillouin function – see the dashed line in Fig. S1 for an ideal paramagnet at *T* = 2 K. Deviations of the experimental data from the paramagnetic behavior are barely noticeable, and only for the lowest temperatures, and can be ascribed to the presence of a weak antiferromagnetic interaction. This is corroborated by the *T*-dependence of the magnetic susceptibility χ. As shown by the solid line in the inset of Fig. S1, the susceptibility data can be fitted above 2 K to a Curie-Weiss law $\chi = g^2 \mu_B^2 s(s + 1)/[3k_B (T − \Theta)]$, obtaining a negative, though small, $\Theta = − 0.3$ K, which suggests that the Gd^{3+} moments are weakly antiferromagnetically correlated in the paramagnetic phase.

The top panel of **Figure 2** shows the measured low-temperature heat capacity *C* as a function of temperature for several applied fields. A sharp lambda-like peak can be observed in the zero-field data for $T_{C1} \approx 0.8$ K, denoting the presence of a phase transition, which is accompanied by a smooth, tiny feature at $T_{C2} \approx 0.4$ K. The magnetic origin of

both anomalies is proved by the fact that external applied fields fully suppress them.[20] In agreement with $M(T,B)$, the analysis of the field-dependent C reveals that magnetic interactions between the Gd^{3+} spin centers are relatively weak, since an applied field $B = 1$ T is sufficient for fully decoupling all spins. As shown in Fig. 2, the calculated Schottky contributions (solid lines) for the field-split levels of the non-interacting $s = 7/2$ multiplet nicely account for the magnetic contribution C_m to the experimental heat capacity. For $T \geq 7$ K, a large field-independent contribution appears, which can be attributed to the lattice phonon modes of the crystal. The dashed line in the top panel of Fig. 2 represents a fit to this contribution, with the well-known Debye function yielding a value of $\Theta_D = 168$ K for the Debye temperature, which is remarkably large for molecular[21] and MOF[15] materials, denoting a relatively rigid lattice. Larger Θ_D implies correspondingly lower lattice entropy in the low-temperature region, ultimately favoring the MCE. From the experimental heat capacity the temperature dependence of the magnetic entropy $S_m(T)$ is derived by integration, i.e.,

$$S_m(T) = \int_0^T \frac{C_m(T)}{T} dT, \tag{1}$$

where C_m is obtained by subtracting the lattice contribution to the total C measured. The so-obtained $S_m(T)$ is shown in the bottom panel of Fig. 2 for the corresponding applied fields. For $B = 0$, the lack of experimental C_m for $T \leq 0.3$ K has been taken into account by matching the limiting S_m at high temperature with the value obtained from the in-field data. One can notice that there is a full entropy content of $R\ln(8) \cong 17.3$ J mol^{-1} K^{-1} $\cong 59.0$ J kg^{-1} K^{-1} per mole Gd^{3+} involved, as expected from $R\ln(2s + 1)$ and $s = 7/2$, where R is the gas constant and the molecular mass is $m = 292.30$ g mol^{-1}.
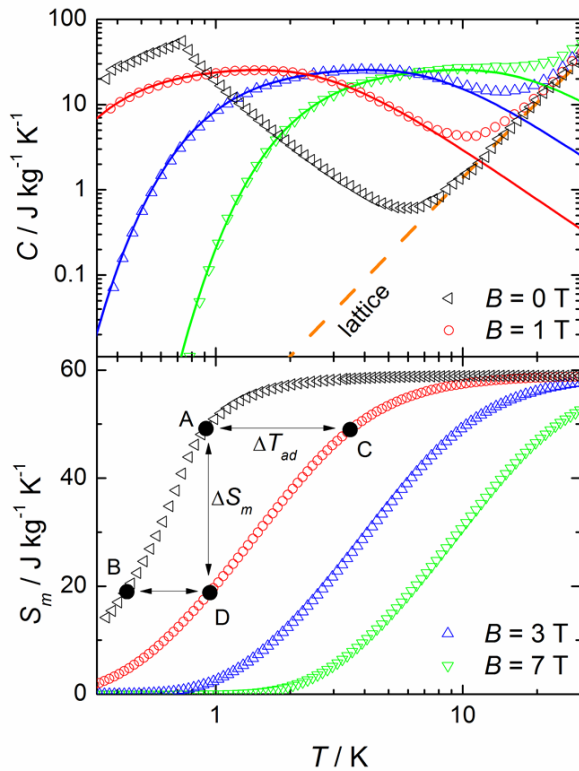
← *Figure 2.* Top: temperature-dependence of the heat capacity C, collected for selected B values, as labeled. Solid thick lines are the calculated Schottky contributions for the corresponding B, and dashed line is the fitted lattice contribution. Bottom: temperature-dependence of the experimental magnetic entropy S_m for several B, as obtained from the magnetic contribution C_m to the total heat capacity. Highlighted examples of magnetic entropy change ΔS_m (for A ↔ D) and adiabatic temperature changes ΔT_{ad} (for A ↔ C and B ↔ D).

Next, we indirectly evaluate the MCE of Gd(HCOO)$_3$ from the experimental data presented so far. From the bottom panel of Fig. 2, we obtain the magnetic entropy changes $\Delta S_m(T,\Delta B)$ for different applied field changes $\Delta B = B_f - B_i$. The so-obtained results are depicted in **Figure 3**. A similar set of data can also be derived from an isothermal process of magnetization by employing the Maxwell relation, i.e., $\Delta S_m(T,\Delta B) = \int_{B_i}^{B_f} \left[\partial M(T,B)/\partial T \right]_B dB$. From the experimental $M(T,B)$ data in Fig. S1, we then obtain curves that rather beautifully agree with the corresponding results previously derived from heat capacity – see the top panel of Fig. 3. Furthermore, to a cooling process under adiabatic conditions, one naturally associates a temperature change whose estimate is made feasible by knowing C and thus S_m. The bottom panel of Fig. 3 shows $\Delta T_{ad}(T,\Delta B)$, where T denotes the final temperature of the adiabatic cooling, e.g., going from C($T = 3.4$ K, $B = 1$ T) to A($T = 0.95$ K, $B = 0$) in Fig. 2. A far more elegant and reliable method for determining the MCE is by directly measuring $\Delta T_{ad}(T,\Delta B)$ under quasi-adiabatic conditions.[22] Following the procedure described in the Supporting Information, we have carried measurements for the experimental conditions corresponding to the magnetization (A $\rightarrow$ C) and demagnetization (D $\rightarrow$ B) processes highlighted in Fig. 2. Starting from $T_i = 0.98$ K, the result, depicted in **Figure S2**, yields ($T_i \rightarrow T \rightarrow 3.45$ K for $0 \rightarrow B \rightarrow 1$ T) and ($T_i \rightarrow T \rightarrow 0.47$ K for 1 T $\rightarrow B \rightarrow 0$), thus corresponding to $\Delta T_{ad} = 2.47$ K and 0.51 K for magnetization and demagnetization, respectively, in nice agreement with what is obtained from the entropy data (see Figure 2).
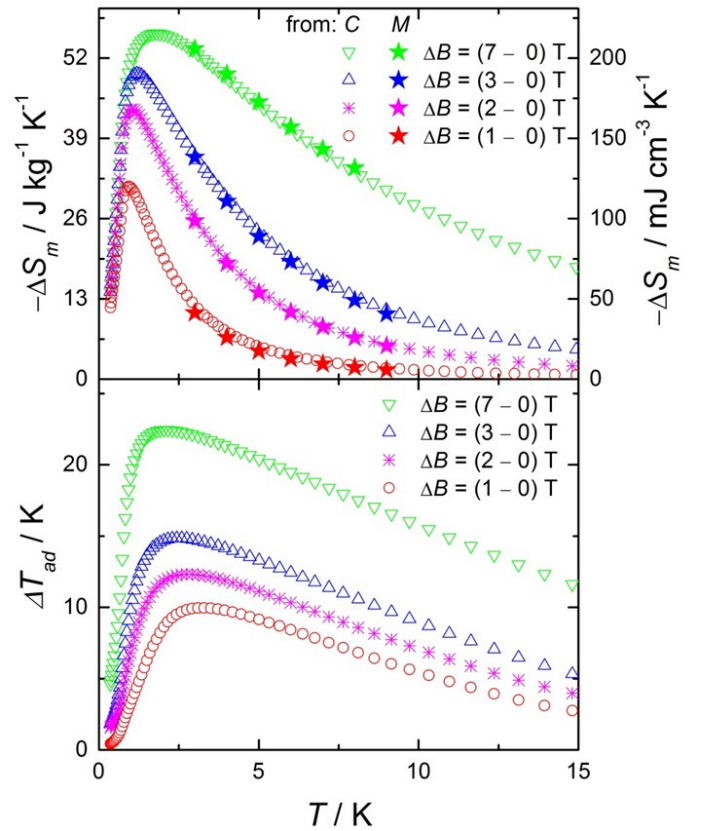
Figure 3 →. Top: temperature-dependence of the magnetic entropy change ΔS_m, as obtained from magnetization and heat capacity data (see Figures S1 and 2, resp.) for the indicated applied-field changes ΔB. Vertical axis reports units in J kg^{-1} K^{-1} (left) and volumetric mJ cm^{-3} K^{-1} (right). Bottom: temperature-dependence of the adiabatic temperature change ΔT_{ad}, as obtained from heat capacity data for the indicated ΔB.

The MCE of Gd(HCOO)$_3$ is exceptionally large, especially in comparison with other molecule-based magnetic refrigerants, as summarized in **Table 1** for three representative examples from the recent literature. All of them are characterized by a pronounced maximum of the MCE at $T^{(max)} \simeq 1$ K for $\Delta B = 2$ T, as for Gd(HCOO)$_3$. The choice of $\Delta B = 2$ T is dictated by the fact that, for widespread applications, the interest is chiefly restricted to applied fields which can be produced with permanent magnets. In Table 1, the maximum entropy changes $-\Delta S_m^{(max)}$ are reported per unit volume. Although these units are not often used, they are better suited for assessing the implementation of the refrigerant material in a designed apparatus.[23] On this point, one could correctly argue that the MCE of molecule-based refrigerant materials is disfavored by their typically low mass density, ρ. However, Gd^{3+} centers in Gd(HCOO)$_3$ are interconnected only by short and extremely lightweight HCOO$^-$ ligands, resulting in a relatively large $\rho = 3.86$ g cm^{-3}. Ultimately, this enhances the MCE, favored by a larger weight of magnetic elements with respect to non-magnetic ones, which act passively. To the best of our knowledge, no other molecule-based refrigerant material has a MCE as large as in Gd(HCOO)$_3$: $-\Delta S_m^{(max)} \simeq 155$ mJ cm^{-3} K^{-1} and 189 mJ cm^{-3} K^{-1} for $\Delta B = (2-0)$ T and $(7-0)$ T, respectively, as shown in Figure 3. This comparison would not be complete without assessing the efficiency of refrigeration for every selected material. This is accomplished by estimating the relative cooling power (RCP),[23] defined as the product of $-\Delta S_m^{(max)}$ and the full width at half maximum of the corresponding $-\Delta S_m(T)$ curve, i.e., δT_{FWHM}. Among the other molecule-based refrigerants in Table 1, Gd(HCOO)$_3$ with RCP = 522.4 mJ cm^{-3} proves once again to be the unbeatable choice. Lastly, we extend this comparison to also include gadolinium gallium garnet (GGG), which is *the* reference magnetic refrigerant material for the 1 K < T < 5 K range.[24,25] Indeed, its functionality is commercially exploited, also owed to its large $\rho = 7.08$ g cm^{-3}, which contributes to provide record values for $-\Delta S_m^{(max)} \simeq 145$ mJ cm^{-3} K^{-1} and RCP = 478.5 mJ cm^{-3} for the same applied field change of 2 T. As can be seen in Table 1, these values are close to, but still lower than, the reported ones for Gd(HCOO)$_3$.

	ρ g cm^{-3}	$-\Delta S_m^{(max)}$ mJ K^{-1} cm^{-3}	$T^{(max)}$ K	δT_{FWHM} K	RCP mJ cm^{-3}	Ref.
Gd(HCOO)$_3$	3.856	168.5	1.1	3.1	522.4	this work
[{Gd(OAc)$_3$(H$_2$O)$_2$}$_2$]·4H$_2$O	2.038	66.5	0.9	3.2	212.8	[8]
[Gd(HCOO)(OAc)$_2$(H$_2$O)$_2$]	2.397	88.9	0.9	3.2	284.5	[15]
Gd$_2$(fum)$_3$(H$_2$O)$_4$·3H$_2$O	2.515	45.3	1.0	2.4	108.7	[12]
Gd$_3$Ga$_5$O$_{12}$ (GGG)	7.080	145.0	1.2	3.3	478.5	[23]

Table 1. Parameters of selected refrigerant materials with a high magnetocaloric effect at liquid-helium temperatures and for the applied field change $\Delta B = (2-0)$ T. From left to right: ρ, mass density; $-\Delta S_m^{(max)}$, maximum magnetic entropy change; $T^{(max)}$, temperature of the corresponding $-\Delta S_m^{(max)}$; δT_{FWHM}, full width at half maximum of the corresponding $-\Delta S_m(T)$; RCP, relative cooling power; corresponding reference.

Concluding, we experimentally determine the magnetocaloric effect of the Gd(HCOO)$_3$ metal-organic framework material. Under quasi-adiabatic conditions, sub-Kelvin direct measurements of the temperature change corroborate the results inferred from indirect methods. The comparison of gadolinium formate with other excellent magnetic refrigerants for liquid-helium temperatures, such as the benchmark GGG, reveals that Gd(HCOO)$_3$ has an unprecedently large MCE. Our observations are interpreted as the result of a light and compact structural framework promoting very weak magnetic correlations between the Gd^{3+} spin centers.

Finally, we foresee that synthetic and technological strategies, already developed for the surface deposition of MOF materials, could ultimately facilitate the integration and exploitation of Gd(HCOO)$_3$ within molecule-based microdevices for on-chip local refrigeration.[26]

Experimental

Single-crystal structure determination: Data were obtained from a colorless block on an Agilent Technologies SuperNova diffractometer with a Mo microsource ($\lambda = 0.71073$ Å). Cell refinement, data reduction and absorption corrections were performed with Crysalis Pro.[27] Coordinates from the Yttrium structure (code LOSKUA[28]) were used as initial solution, and refinement on F^2 was done with SHELXTL.[29] CCDC: Crystallographic and refinement parameters are summarized in **Table S1**, while full data (excluding structure factors) have been deposited with the Cambridge Crystallographic Data Centre as supplementary publication No. CCDC-914467.

Magneto-thermal characterization: Magnetization measurements down to 2 K and heat capacity measurements using the relaxation method down to ≈ 0.35 K were carried out on powder samples by means of commercial setups (QDMPMS- XL and QD-PPMS, resp.) for $0 < B < 5$ T and $0 < B < 7$ T, respectively. Direct measurements of the MCE were performed on a powder sample using a sapphire plate to which a Cernox (CX-1010) resistance thermometer is attached, installed in the same setup employed for heat capacity.

Notes and references

[1] For a recent review see, e.g., M. Evangelisti, E. K. Brechin, *Dalton Trans.* **2010**, *39*, 4672 and references therein.

[2] See, e.g., R. Sessoli, *Angew. Chem. Int.-Ed.* **2012**, *51*, 43.

[3] F. Torres, J. M. Hernández, X. Bohigas, J. Tejada, *Appl. Phys. Lett.* **2000**, *77*, 3248.

[4] Yu. I. Spichkin, A. K. Zvezdin, S. P. Gubin, A. S. Mischenko, A. M. Tishin, *J. Phys.D: Appl. Phys.* **2001**, *34*, 1162.

[5] M. Affronte, A. Ghirri, S. Carretta, G. Amoretti, S. Piligkos, G. A. Timco, R. E. P. Winpenny, *Appl. Phys. Lett.* **2004**, *84*, 3468.

[6] M. Evangelisti, A. Candini, A. Ghirri, M. Affronte, E. K. Brechin, E. J. L. McInnes, *Appl. Phys. Lett.* **2005**, *87*, 072504.

[7] M. Evangelisti, A. Candini, M. Affronte, E. Pasca, L. J. de Jongh, R. T. W. Scott, E. K. Brechin, *Phys. Rev. B* **2009**, *79*, 104414.

[8] M. Evangelisti, O. Roubeau, E. Palacios, A. Camón, T. N. Hooper, E. K. Brechin, J. J. Alonso, *Angew. Chem. Int.-Ed.* **2011**, *50*, 6606.

[9] S. K. Langley, N. F. Chilton, B. Moubaraki, T. Hooper, E. K. Brechin, M. Evangelisti, K. S. Murray, *Chem. Sci.* **2011**, *2*, 1166.

[10] M.-J. Martínez-Pérez, O. Montero, M. Evangelisti, F. Luis, J. Sesé, S. Cardona-Serra, E. Coronado, *Adv. Mater.* **2012**, *24*, 4301.

[11] a) E. Manuel, M. Evangelisti, M. Affronte, M. Okubo, C. Train, M. Verdaguer, *Phys. Rev. B* **2006**, *73*, 172406; b) M. Evangelisti, E. Manuel, M. Affronte, M. Okubo, C. Train, M. Verdaguer, *J. Magn. Magn. Mater.* **2007**, *316*, e569.

[12] L. Sedláková, J. Hanko, A. Orendčov, M. Orendáč, C. L. Zhou, W. H. Zhu, B. W. Wang, Z. M. Wang, S. Gao, *J. Alloys Compd.* **2009**, *487*, 425.

[13] R. Sibille, T. Mazet, B. Malaman, M. François, *Chem. Eur. J.* **2012**, *18*, 12970.

[14] F.-S. Guo, Y.-C. Chen, J.-L. Liu, J.-D. Leng, Z.-S. Meng, P. Vrábel, M. Orendáč, M.-L. Tong, *Chem. Commun.* **2012**, *48*, 12219.

[15] G. Lorusso, M. A. Palacios, G. S. Nichol, E. K. Brechin, O. Roubeau, M. Evangelisti, *Chem. Commun.* **2012**, *48*, 7592.

[16] W. F. Giauque, D. P. MacDougall, *Phys. Rev.* **1933**, *43*, 768.

[17] A. Pabst, *J. Chem. Phys.* **1943**, *11*, 145.

[18] Gd(HCOO)$_3$ crystallizes in space group $R3m$ with $a = b = 10.4583(4)$ Å, $c = 3.9869(3)$ Å, $\alpha = \beta = 90°$, $\gamma = 120°$ and $Z = 3$. The distance between nearest and next-nearest Gd neighbors is 3.98 Å and 6.19 Å, respectively. CCDC-914467 contains the supplementary crystallographic data, which can be obtained free of charge from the Cambridge Crystallographic Data Centre.

[19] J. D. Cashion, D. B. Prowse, A. Vas, *J. Phys. C: Solid State Phys.* **1973**, *6*, 2611.

[20] We refrain from discussing the magnetic ordering mechanism any further since this topic exceeds the scope of this article and its full comprehension requires additional measurements, whose results will be exhaustively presented elsewhere.

[21] See, e.g., M. Evangelisti, F. Luis, L. J. de Jongh, M. Affronte, *J. Mater. Chem.* **2006**, *16*, 2534, and references therein.

[22] a) L. Tocado, Ph. D. Thesis, Universidad de Zaragoza, **2008**; b) L. Tocado, E. Palacios, R. Burriel, *J. Magn. Magn. Mater.* **2005**, *290-291*, 719.

[23] See, e.g., A. M. Tishin, Y. I. Spichkin, *The magnetocaloric effect and its applications*, Taylor & Francis, London **2003**.

[24] B. Daudin, R. Lagnier, B. Salce, *J. Magn. Magn. Mater.* **1982**, *27*, 315.

[25] T. Numazawa, K. Kamiya, T. Okano, K. Matsumoto, *Physica B* **2003**, *329-333*, 1656.

[26] G. Lorusso, M. Jenkins, P. González-Monje, A. Arauzo, J. Sesé, D. Ruiz-Molina, O. Roubeau, M. Evangelisti, *Adv. Mater.* – DOI: 10.1002/adma.201204863.

[27] Crysalis Pro, Agilent Technologies Ltd., Yarnton, UK, **2011**.

[28] V. A. Trunov, V. A. Kudryashev, A. P. Bulkin, V. A. Ulyanov, A. A. Loshmanov, N. G. Furmanova, O. Antson, P. Hiismäki, H. Mtka, H. Pöyry, A. Tlitta, *Solid. State. Commun.* **1986**, *59*, 95.

[29] G. M. Sheldrick, *Acta Cryst. A* **2008**, *64*, 112.